Loss of Effector Function of Human Cytolytic T Lymphocytes is Accompanied by Major Alterations in N- and O-Glycosylation*

Aristotelis Antonopoulos[‡], Nathalie Demotte[§], Vincent Stroobant[§], Stuart M. Haslam[‡], Pierre van der Bruggen[§], and Anne Dell[‡1]

From the [‡]Division of Molecular Biosciences, Imperial College London, SW7 2AZ, UK, and [§]Ludwig Institute for Cancer Research, WELBIO, and Université catholique de Louvain, de Duve Institute, 74 av. Hippocrate, P.O. Box B1-7403, B-1200 Brussels, Belgium

*Running title: *Glycomics on Human Cytolytic T Lymphocytes*

To whom correspondence should be addressed: Anne Dell, Division of Molecular Biosciences, Imperial College London, South Kensington Campus, SW7 2AZ, UK, Tel.: +44 (0)207 5945219; E-mail: a.dell@imperial.ac.uk

Keywords: CTLs; galectin-3; N-glycans; MALDI-TOF; TCR; tumor microenvironment

Background: Most human tumors escape immune system because of the immunosuppressive tumor microenvironment.
Results: N-acetyllactosamine units, the ligands for galectin-3, and branching on N-linked glycans are increased in the recently activated cytolytic T lymphocytes.
Conclusion: The increased galectin-3-lattices decrease the motility of key surface glycoproteins.
Significance: Loss of effector functions on cytolytic T lymphocytes may be linked to reduced motility of surface glycoproteins.

SUMMARY

Most human tumors are not eliminated by the immune system and therapeutic vaccination shows poor results, a fact that can be explained, at least partially, by an immunosuppressive tumor microenvironment which is abundant in galectin-3. On cytolytic T lymphocyte (CTL) clones, maintained in culture by regular stimulation, recently activated CTLs present low effector functions. However, these functions are restored after a short treatment with LacNAc. The latter, which is in agreement with the glycoprotein-galectin lattice concept involving reduced motility, poses the question why galectin-3 ligands improve effector functions. We employed ultra-sensitive MALDI-TOF-MS on resting and recently activated CTL clones, combined with various glycosidase digestions and GC-MS linkage analyses. Our results showed that compared with the resting CTLs, the N-glycans of the recently activated CTLs consisted of: (i) larger LacNAc oligomers of which a significant portion was longer than four-units; (ii) more multi-antennary structures. Interestingly, our results showed that the poly-LacNAc appeared to be equally distributed on all available N-glycan branches and not selectively enriched on a specific branch. The above structural alterations in the recently activated CTLs are expected to increase the galectin-3-LacNAc lattices and multivalent interactions and therefore reduce the motility of surface glycoproteins, such as the TCR. These findings suggest that the loss of effector functions on CTLs may be linked to reduced motility of surface glycoproteins. In addition, our results showed that recently activated CTLs had a reduced abundance of NeuAcα2,6-linked N-glycans and an increased abundance of disialylated core 1 and monosialylated core 2 O-glycan structures.

Human tumors are usually not spontaneously eliminated by the immune system and therapeutic vaccination of cancer patients with defined antigens is followed by tumor regressions only in a small minority of patients (1, 2). The poor vaccination effectiveness could be explained by an immunosuppressive tumor microenvironment. Because T cells that do infiltrate tumor metastases have an impaired ability to lyse target cells or to secrete cytokines when they are stimulated *ex vivo*, *i.e.* tested on

untreated and uncultured samples (3-7), many researchers are trying to decipher the underlying immunosuppressive mechanisms.

We suggested that extracellular galectin-3, abundant in solid tumor and carcinoma ascites, impairs human tumor-infiltrating T lymphocyte $(TIL)^2$ function (8). The motility of surface molecules, such as the T-cell receptor (TCR), which are necessary for T cell activation and function, can be reduced because they are trapped in a lattice of glycoproteins clustered by extracellular galectin-3 (9). Several of our results support this hypothesis. First, human tumor-infiltrating $CD8^+$ T lymphocytes (TIL) from diverse histological origins, in contrast with $CD8^+$ blood cells, have an impaired ability to secrete IFN-γ upon *ex vivo* stimulation (6). We documented by FRET, the physical dissociation of TCR and CD8 on these TIL. Second, TIL harbour surface galectin-3 which can be detached by treatment of $CD8^+$ TIL with an anti-galectin-3 antibody. A 2-h treatment of TIL with this antibody, followed by overnight stimulation with beads coated with anti-CD3 antibodies, that mimic an antigenic stimulation, boosted their secretion of IFN-γ (6). Third, two galectin ligands, *N*-acetyllactosamine (Galβ1,4GlcNAc; LacNAc) and GCS-100, a modified citrus pectin, detached galectin-3 from TIL, promoted co-localization of TCR and CD8 co-receptor and increased their cytotoxicity and their ability to secrete IFN-γ upon stimulation (6). It has to be noted that both galectin ligands are also able to detach galectin-1 from cells.

We also analysed the effect of galectin ligand LacNAc on cytolytic T lymphocyte (CTL) clones maintained in culture by regular antigenic stimulation, *i.e.* every two weeks. Compared with resting CTL collected 14 days after the last stimulation, recently activated CTL that were collected 4 days after stimulation secreted low levels of IFN-γ upon a further antigenic stimulation (8). We documented by FRET and by confocal microscopy the physical dissociation of TCR and CD8 at the surface of recently activated lymphocytes whereas TCR and CD8 were co-localized on most of the resting cells. In agreement with the hypothesis of a glycoprotein-galectin lattice on recently activated CTL, a short treatment of these CTL with LacNAc increased the proximity between TCR with the CD8 and restored their ability to secrete high levels of IFN-γ.

Experiments in mice models have revealed the influence of N-glycans on T cell activation. Firstly, T cells from mice lacking *N*-acetylglucosaminyltransferase V (Mgat5), an enzyme essential for the generation of complex tetra-antennary N-glycans, have a lower activation threshold than T cells from wild type-mice. The tetra-antennary N-glycans can carry poly-LacNAc chains, the natural ligands of galectin-3. Mgat5-deficient mice showed evidence of immune dysfunction by increased sign of proliferative glomerulonephritis and were more susceptible to develop autoimmune encephalomyelitis (9). Secondly, T cells from mice lacking β1,3-*N*-acetylglucosaminyltransferase 2 have reduced poly-LacNAc on their N-glycans and were much more sensitive to activation upon stimulation with anti-CD3 coated beads (10). Finally, Kuball *et al*. introduced mutations in a TCR coding sequence that destroy N-glycosylation sites (11). These modified sequences were grafted in polyclonal T cells, which acquire a better avidity for the antigen recognized by the grafted TCR than T cells carrying the wild-type TCR. The authors proposed that glycosylation affects the flexibility, movement, and interactions of surface molecules, but it cannot be excluded that these mutations also affect the number of galectin ligands and the possibility to form TCR-galectin lattices.

Why do galectin ligands improve effector functions of human TIL and CTL clones? Our working hypothesis is that, as a consequence of antigen-stimulated activation of T cells, the expression of enzymes of the N-glycosylation pathway is modified, and this changes the structures of N-glycans exposed at the cell surface. In agreement with that hypothesis, when resting CTL were stimulated in the presence of swainsonine, a inhibitor of α-mannosidase II which is involved in the N-glycosylation pathway, recently activated CTL collected at day 4 after stimulation, compared to untreated cells, showed a higher TCR-CD8 FRET efficiency and a higher ability to release IFN-γ upon antigenic stimulation (8). We surmise that the recently activated TIL, compared to resting T cells, harbour a set of glycans that are either more numerous or better ligands for galectin-3, and possibly for other galectins, such as galectin-1. *In vivo*, tumor cells, macrophages, and possibly activated T cells can secrete galectin-3. In *in vitro* cultures of CTL clones, galectin-3 can be

secreted by the tumor cells used as stimulators, the immortalized B cells used as feeder cells, and possibly by the activated T cells themselves. Indeed, expression of galectin-3 is increased after murine T cell activation by the mitogen ConA. Also, galectin-3 secretion is enhanced in response to calcium ionophore when T cells are previously activated (12).

N-glycans harboured by murine splenocyte T cells have been previously compared with those found at the surface of splenocyte T cells, which were activated by anti-CD3 antibody and collected three days later. Activation resulted in a decreased expression of the sialyltransferase ST6Gal1 and increased expression of the galactosyltranferase α1,3GalT (13). Accordingly, activation resulted in reduction of sialylated biantennary N-glycans carrying the terminal NeuGcα2,6Gal sequence, and a corresponding increase in glycans carrying the Galα1,3Gal sequence. Murine T cells, however, are not good models for potential galectin-mediated processes in the human immune system because they are poor in tri- and tetra-antennary poly-LacNAc glycans (14).

Here, we characterised global changes in N- and O-glycans of two human CTL clones that were analysed either in a resting state or four days after antigenic stimulation. Applying ultra-sensitive matrix-assisted laser desorption-ionisation time-of-flight mass spectrometry (MALDI-TOF-MS), combined with various glycosidase digestions and gas chromatography (GC) -MS linkage analyses, we present direct evidence that galectin-3-ligands in recently activated human CTLs, compared with the resting state CTLs, are increased. N-glycans of recently activated CTLs exhibited poly-LacNAc chains of which a portion was found longer than four LacNAc units. Moreover, recently activated CTL clones present more branched (multi-antennary) N-glycans. Differences in the non-reducing N-glycan terminal epitopes and O-glycan structures are also discussed.

EXPERIMENTAL PROCEDURES

CTL clones and stimulation conditions— Anti-MAGE-3.A1 CTL clones LB2586-7/1F3.2 (clone F3.2) and LAU147-810/A10 (clone A10) were described previously (8). Every two weeks, stimulation was performed as described. LacNAc was purchased from Carbosynth.

Antigen recognition assays for CTL clones— CTL clones (10,000) were stimulated for 20 h in round-bottomed microwells, in 100 µl of Iscove's modified Dulbecco medium (IMDM), 10% human serum (HS), 0.24 mM L-asparagine, 0.55 mM L-arginine, 1.5 mM L-glutamine (AAG) with 10,000 HLA-A1 irradiated allogeneic Epstein Barr virus immortalized B (EBV-B) cells previously incubated with MAGE-3 peptide EVDPIGHLY. Amounts of IFN-γ secreted after overnight co-culture were measured by ELISA using Biosource Cytoset reagents (Invitrogen). When indicated, CTL clones (10,000) were previously incubated for 2 h in round-bottomed microwells, in 50 µl of IMDM, 10% HS, AAG with 2 mM LacNAc before adding the stimulator cells.

Cell pellets— Cells were collected and washed. Dead cells were removed by a depletion selection strategy, using the Dead Cell Removal Kit (AutoMACS system, Miltenyi Biotec). Cells were then washed and remaining EBV-B cells were removed by a positive selection strategy using magnetic beads coated with anti-CD19 (AutoMACS system, Miltenyi Biotec). Cells were finally washed in PBS, dry pelleted and stored at -80 °C.

Processing of CTL clones to obtain N- and O-glycans— All human CTL clones (clones A10 and F3.2) were treated as described previously (15). Briefly, each CTL clone (~20 million) was subjected to sonication in the presence of detergent (CHAPS), reduction in 4 M guanidine-HCl (Pierce, Cramlington, Northumberland, UK), carboxymethylation and trypsin digestion. The digested glycoproteins were then purified by C_{18}-Sep-Pak (Waters Corp, Hertfordshire, UK). N-glycans were released by peptide N-glycosidase F (E.C. 3.5.1.52; Roche Applied Science, Burgess Hill, UK) digestion while O-glycans were released by reductive elimination. Released N- and O-glycans were permethylated using the sodium hydroxide procedure and purified by C_{18}-Sep-Pak. The results shown are representative of three independent experiments.

Sialidase digestions— Cleavage of the all sialic acids (NeuAc) or of α2,3 specific from the CTL clones A10 and F3.2 was performed with a sialidase-A (*Arthrobacter ureafaciens*; E.C. 3.2.1.18; Prozyme, GK80040) and sialidase-S (*Spectrococcus pneumoniae*; E.C. 3.2.1.18; Prozyme, GK80020) digestions respectively. Released N-glycans were incubated in 200 µl of 50 mM sodium acetate (37 °C, pH 5.5). 170 mU of the enzyme were added to the sample for 24 h.

Remove of fucose residues— Removal of all fucose residues attached to antennae of N-glycans was performed with hydrofluoric acid (HF) treatment. 50 µl of HF (48% v/v) was added to the sample for 48 h at 4 °C. The reaction was terminated by drying the sample under a gentle stream of nitrogen.

Galactosidase digestion— Cleavage of galactose residues was performed with a β(1-3,4)-galactosidase from bovine testis (E.C. 3.2.1.23; Prozyme, GKX-5013). Released N-glycans were incubated in 200 µl of 50 mM ammonium acetate (pH 4.6, 37 °C) for 24 h. 10 mU of the enzyme was added with a fresh aliquot being added after 12 h.

Hexosaminidase digestion— Cleavage of β-*N*-acetylglucosamine residues was performed with a β-*N*-acetylhexosaminidase (*Streptococcus pneumoniae*; E.C. 3.2.1.52; Prozyme, GK80050). Released N-glycans were incubated in 200 µl of 50 mM sodium formate (pH 5.0, 37 °C) for 24 h. 80 mU of the enzyme was added with a fresh aliquot being added after 12 h.

Endo-β-galactosidase digestion— Endo-β-galactoside (*Escherichia freundii*; E.C. 3.2.1.103; Seikagaku Corp, AMS Biotechnology Ltd, 100455) digestion was carried out in 200 µl of sodium acetate (pH 5.8, 37 °C). 20 mU of the enzyme were added to the sample for 48 h with a fresh aliquot being added after 24 h.

E. freundii endo-β-galactosidase hydrolyzes the internal β-galactosidic linkages of both the type 1 and type 2 linear polylactosamine chains having as a minimum structural requirement the structure GlcNAcβ1-3Galβ1-3GlcNAc (or β1-4GlcNAc for type 2) (16, 17). The action of *E. freundii* endo-β-galactosidase is inhibited by fucosylation of residues in close proximity to the internal β-galactosidic linkage (16, 17). For example, for the mono-fucosylated structure Galβ1-4GlcNAcβ1-3Galβ1-4(Fucα1-3)GlcNAc, the cleavage at the β-galactose residue is inhibited by the fucose on the GlcNAc residue.

Mass spectrometry— MS data were acquired using either a Voyager-DE STR MALDI-TOF or a 4800 MALDI-TOF/TOF (Applied Biosystems, Darmstadt, Germany) mass spectrometer. MS/MS data were acquired using a 4800 MALDI-TOF/TOF mass spectrometer. Permethylated samples were dissolved in 10 µl of methanol and 1 µl of dissolved sample was premixed with 1 µl of matrix (20 mg/ml 2,5-dihydroxybenzoic acid (DHB) in 70% (v/v) aqueous methanol), spotted onto a target plate and dried under vacuum. For the MS/MS studies the collision energy was set to 1 kV, and argon was used as collision gas. The 4700 Calibration standard kit, calmix (Applied Biosystems), was used as the external calibrant for the MS mode and [Glu1] fibrinopeptide B human (Sigma-Aldrich) was used as an external calibrant for the MS/MS mode.

Analyses of MALDI data— The MS and MS/MS data were processed using Data Explorer 4.9 Software (Applied Biosystems). The processed spectra were subjected to manual assignment and annotation with the aid of a glycobioinformatics tool, GlycoWorkBench (18). The proposed assignments for the selected peaks were based on ^{12}C isotopic composition together with knowledge of the biosynthetic pathways. The proposed structures were then confirmed by data obtained from MS/MS and linkage analysis experiments.

Gas-chromatography mass spectrometry (GC-MS) linkage analysis— Partially methylated alditol acetates (PMAA) were prepared as previously described (15). Linkage analysis of PMAA was performed on a Perkin Elmer Clarus 500 instrument fitted with a RTX-5 fused silica capillary column (30 m × 0.32 mm i.d.; Restek Corp.). The sample was dissolved in ~20-50 µl of hexanes and injected manually (2-3 µl). Injector temperature was set at 250 °C. PMAA were eluted with the following linear gradient oven: initially the oven temperature was set at 65 °C for 1 min, heated to 290 °C at a rate of 8 °C per min, held at 290 °C for 5 min and finally heated to 300 °C at a rate of 10 °C per min.

RESULTS

CTL clones A10 and F3.2 were both directed against MAGE-3 peptide EVDPIGHLY presented by HLA-A1. They were expanded *in vitro* by stimulation every 14 days, using peptide-pulsed HLA-A1 cells. To assess the effector capability of the CTL at various points of the stimulation cycle, cells were collected at either 4 days (activated) or 14 days (resting) after antigenic stimulation and co-culturing with peptide-pulsed HLA-A1 cells. Amounts of IFN-γ secreted by the CTL were estimated by ELISA in the supernatant of overnight co-cultures. Compared to CTL collected on day 0, CTL collected on day 4 secreted lower levels of IFN-γ upon re-stimulation (Fig. 1 and supplemental

Fig. S1). But, when recently activated CTLs, collected on day 4, were treated for 2 h with galectin ligand LacNAc, their ability to secrete high levels of IFN-γ upon re-stimulation was restored. On the contrary, LacNAc treatment did not affect IFN-γ secretion on resting CTL clones (supplemental Fig. S2). Extracellular galectin-1 and galectin-3 were both detected at the surface of recently activated CTL. The latter CTL contains more galectin-1 than the resting CTL. No detectable galectin-3 was found on the resting CTL. A treatment of 2 h with LacNAc, on the recently activated CTL, partially detached both galectins (supplemental Fig. S3). To analyse the N- and O-glycans at the cell surface of resting and activated CTL, cells were collected at the indicated time, dead cells and stimulator cells were removed using a depletion strategy, and CTL were subsequently pelleted and frozen at -80 °C.

Glycomic analysis of CTLs revealed differences on N- and O-glycans— The N-glycomic profile of resting CTL clone A10 consisted of high mannose and complex structures (Fig. 2*A*). Compositional and MALDI-TOF-TOF MS/MS analyses suggested that the latter were mainly core fucosylated and non-bisected, and corresponded to bi-, tri- and tetra-antennary N-glycan structures occasionally extended with LacNAc repeats. The non-reducing ends of these glycans either remained unmodified (*m/z* 2244, 2489, 2938, 4490) or were further modified, mainly with terminal NeuAc residues (*m/z* 2605, 3416, 4402, 5300). The sLe^x terminal epitope was also detected in bi-antennary (*m/z* 3140, 3314) and tri-antennary (*m/z* 3951 and 4125) N-glycan structures. However, it was of low abundance compared with other terminal structures.

The N-glycomic profile of recently activated CTL clone A10 exhibited similar N-glycans to the resting state CTLs, but with the following differences being observed (Fig. 2*B*): (i) N-glycans with extended poly-LacNAc structures were of higher abundance, compared with the resting state, resulting in higher molecular weight N-glycan structures reaching up to 7000 mass units; (ii*)* sLe^x terminated glycans were of higher abundance. For example comparing the ratios of *m/z* 3140 with *m/z* 2966 on both the resting and recently activated states (Fig. 2*A* and *B*), it was concluded that the sLe^x structures in the recently activated state were of higher abundance. In addition, the sLe^x containing N-glycans were overlapped with other most abundant structures. For example, the tri-antennary sLe^x structure detected at *m/z* 3951 (Fig. 2*B*) was observed as a minor peak in the *m/z* 3953-ion cluster that corresponded to a mono-sialylated core fucosylated N-glycan.

The O-glycomic profile of the resting CTL clone A10 exhibited mainly the monosialylated core 1 sequence (*m/z* 895) together with a tiny amount of a non-sialylated core 2 (*m/z* 983) structure (Fig. 3*A*). Recently activated A10 CTLs (Fig. 3*B*) contained, in addition to the core 1 O-glycan at *m/z* 895, disialylated core 1 O-glycans (*m/z* 1256) and a higher abundance of core 2 O-glycans, either unmodified (*m/z* 983) or terminated with one NeuAc residue (*m/z* 1344) or with a Le^x terminal epitope (*m/z* 1157).

The glycomic profiles of resting and recently activated CTL clone F3.2 were similar to the CTL clone A10 structures with complex N-glycans being extended with LacNAc repeats and elaborated with the same terminal epitopes, while O-glycans consisted of core 1 and core 2 structures terminated with NeuAc, Le^x and minor abundances of sLe^x terminal epitopes (supplemental Figs. S4 and S5).

Endo-β-galactosidase digestion revealed differences in the relative abundance of various terminal epitopes and polylactosamine-type N-glycans— The N-glycome of CTL clones A10 and F3.2 suggested differences in the relative abundance of the terminal epitopes and LacNAc repeats. Therefore, we performed an endo-β-galactosidase digestion on the N-glycans of both CTLs (supplemental Fig. S6) with a twofold aim: (i) to verify whether any of the N-glycans of the aforementioned CTLs contained linear polylactosamine chains and (ii) to characterize and reveal any potential differences in the relative abundances on the non-reducing terminal epitopes between resting and recently activated CTLs. The existence of the above should be revealed by the new molecular ions in the low mass region corresponding to antennae fragments released by the enzyme. The low mass permethylated products of the CTL clone A10 in both states (resting and recently activated) are depicted in Fig. 4. Disaccharides released from within the polylactosamine chains gave the signal at *m/z* 518 corresponding to the GlcNAc-Gal sequence (Fig. 4*A* and *B*). The molecular ions at *m/z* 722, 896, 1083 and 1257 were consistent with the terminal sequences Gal-GlcNAc-Gal, Gal-(Fuc)GlcNAc-Gal, NeuAc-

Gal-GlcNAc-Gal and NeuAc-Gal-(Fuc)GlcNAc-Gal respectively which were predicted digestion products of uncapped, fucosylated, sialylated and sLe^x polylactosamine chains respectively. Evidence for the *m/z* 896 and 1257 components being terminated by Le^x and sLe^x epitopes was provided by MALDI-TOF-TOF MS/MS that yielded major fragments at *m/z* 690 and 1051 respectively (data not shown). Molecular ions at *m/z* 967, 1141, 1171 and 1345 were assigned to pauci-mannose N-glycan structures $Man_2GlcNAc_2$, $Man_2GlcNAc$-(Fuc)GlcNAc, $Man_3GlcNAc_2$ and $Man_3GlcNAc$-(Fuc)GlcNAc which did not correspond to fragments released by the endo-β-galactosidase. Moreover, endo-β-galactosidase digestion revealed the presence of disialylated and Vim-2 terminal epitopes in very low abundance (supplemental Fig. S7).

Analysis of the relative abundances of the above terminal epitopes revealed that compared to the resting state, the recently activated CTL clone A10 had higher levels of unmodified, Le^x and sLe^x terminal epitopes and lower levels of sialylated terminal epitopes. Summing-up the relative abundances of all the terminal epitopes at *m/z* 722, 896, 1083 and 1257, we found that compared with the resting state, recently activated CTL clone A10 was characterized by a decrease in the abundance of sialylated LacNAc repeats at *m/z* 1083 (~24%) and an increase in the abundance of unmodified LacNAcs at *m/z* 722 (~10%). Endo-β-galactosidase digestion on CTL clone F3.2 revealed similar abundances to the CTL clone A10 fragments in both states (supplemental Fig. S8). Uncapped, Le^x, sialylated and sLe^x polylactosamine chains characterized the resting and recently activated CTL clone F3.2. Again, compared with the resting state, recently activated CTL clone F3.2 was characterized by a decrease in the abundance of sialylated LacNAc repeats (~36%) and an increase in the abundance of unmodified LacNAcs (~196%). The reduction in glycan complexity on both CTL clones A10 and F3.2 afforded by the endo-β-galactosidase digestion, revealed additional signals that corresponded to N-glycans terminated with multiples of sLe^x epitopes (supplemental Fig. S6). These signals existed in the original glycomic profiles but were in minor abundance and the isotopic cluster of more abundant ions partly masked them. For example, the ions at *m/z* 4761 and 4935 corresponded to tetra-antennary N-glycans with a single and a double sLe^x epitope (supplemental Fig. S6*A* and *B*).

Taken together, the endo-β-galactosidase digestion data on N-glycans of both CTL clones A10 and F3.2 confirmed the presence of polylactosamine chains that remained unmodified or were terminated with Le^x, sialyl and sLe^x epitopes. The data also suggested that, compared with the resting state, in the recently activated state there was an increase in the relative abundance of poly-LacNAc and a decrease in the relative abundance of sialylated terminal epitopes.

Linkage analysis revealed differences in polylactosamine-type abundances— The N-glycans of both the resting and recently activated CTLs contain linear LacNAc units whose abundances appeared to be modified in the resting-activation CTLs cycle. Therefore, in order to express the percent difference of the polylactosamine-type chains between the resting and recently activated CTLs, we performed GC-MS linkage analysis. Comparing the relative abundances of the 3-linked galactose and 4-linked GlcNAc residues (that together make-up the LacNAc unit in poly-LacNAc) between resting and recently activated CTLs, we are able to relatively quantify the different abundance of the LacNAc units between the aforementioned CTLs. Linkage analysis was performed on desialylated N-glycans after digestion with broad specificity sialidase-A. This is because α2,3-linked NeuAc residues potentially could be linked to galactose residues and supplementing the 3-linked galactose from the polylactosamine-type chains. Results from linkage analysis from both CTLs clones are depicted in Table 1. Recently activated CTL clone A10 presented a 121% and 344% increase of the 3-linked galactose and 4-linked GlcNAc abundance respectively compared with resting CTLs, while for the CTL clone F3.2 the increase was 48% and 69% respectively. These data show that in both CTLs the N-glycans in the recently activated state contained more LacNAc chains than in the resting state. Additional linkage data confirmed structural differences between the resting and recently activated CTLs. For example the increase of 3,4-GlcNAc residues on the recently activated CTLs was in accordance with the increase of sLe^x epitopes. This increase was 363% and 29% for the CTL clones A10 and F3.2 respectively (Table 1).

Endo-β-galactosidase digestion revealed differences in multi-branched N-glycans— We next investigated whether there was a difference in the abundance of complex bi-, tri- and tetra-antennary N-glycans between the resting and recently activated CTLs that carry LacNAc repeats. Endo-β-galactosidase digestion on resting CTL clone A10 showed that the most abundant N-glycans carrying LacNAc extensions corresponded to bi-antennary (*m/z* 1836) and to a less extent to tri- (*m/z* 2081 and 2285) and tetra-antennary (*m/*z 2326) N-glycan structures (Fig. 5*A*). On the contrary, recently activated CTL clone A10 showed a decrease in the relative abundance of bi-antennary structures and an increase in the abundance of tri- and tetra-antennary N-glycans (Fig. 5*B*). Summing-up the relative abundances of the ions at *m/z* 1836, 2081, 2285, 2326 and 2530, we found that compared with the resting state, the tri- and tetra-antennary N-glycans (*m/z* 2081, 2285, 2326 and 2530) on the recently activated clone A10 were increased by ~89%. The same decrease of the bi-antennary and increase of tri- and tetra-antennary N-glycans was observed when resting and recently activated CTLs clone F3.2 were compared (supplemental Fig. S9). By similar calculations we found that the tri- and tetra-antennary N-glycans on the recently activated clone F3.2 were increased by ~90%. Taken together, the data suggest that recently activated CTLs contain more branched N-glycans that carry LacNAc chains than the resting CTLs.

More polylactosamine chains are found on recently activated CTLs— All previous experiments showed that the N-glycans exist as multi-branched structures extended with LacNAc repeats and terminated with various epitopes and that all these are modified in the resting-activation CTLs cycle. However, none of above experiments gave a cumulative indication on the length of these LacNAcs repeats. This was an important factor to consider because the binding affinity of galectin-3 is expected to be affected by the length of these LacNAc repeats as well as by the relative abundance of these terminal epitopes. Therefore, we determined the minimum length of the LacNAc chains on the resting and recently activated CTL clone F3.2 and additionally where these poly-LacNAcs were mainly formed, i.e. on bi-, tri-, or tetra-antennary N-glycans (Fig. 6).

We removed all fucose and sialic acid residues substituting the antennae by hydrofluoric acid treatment and by a non-specific sialidase enzymatic digestion, respectively, of the N-glycans of the CTL clone F3.2 leaving only the core-fucose and the LacNAc extensions (Fig. 6*A*, upper structure). Then, performing two cycles of enzymatic digestions with subsequent incubations of β-galactosidase and β-*N*-acetylhexosaminidase, we reduced the N-glycan LacNAc chains of the CTL clone F3.2 by 2 LacNAc repeats. Finally, we incubated the resultant N-glycans with endo-β-galactosidase (Fig. 6*A*, upper structure). The new signals appearing in the spectra, or the ones that were greatly enhanced, corresponded to N-glycans deriving from the above process and their structures depended on the number of LacNAc repeats originally present in each branch (Fig. 6*A*, lower structure).

According to this procedure, most of the N-glycan structures detected on the resting and recently activated CTL clone F3.2 (supplemental Fig. S4*A* and *B*) should be fully digested to the basic N-glycan core structure $Man_3GlcNAc(\pm Fuc)GlcNAc$ (see Fig. 6*A*). Indeed, ions detected at *m/z* 1171 and 1345 corresponded to all complex bi-, tri- and tetra-antennary N-glycans that were extended with up to 2 LacNAc units that were terminated with Le^x, sialic acid and sLe^x epitopes (Fig. 6*B*). Ions at *m/z* 1416 and 1590 corresponded to complex structures where one branch was extended with 4 LacNAc repeats or more. Ions detected at *m/z* 1661 and 1836 corresponded to N-glycans that had two branches that originally contained 4 LacNAc repeats or more. The ions detected at *m/z* 1866, 2111 and 2285 had originally one branch extended with 3 LacNAc repeats and one or two branches (depending if they were bisected or not) with 4 LacNAc repeats or more (Fig. 6*A* and *B*). The ion detected at *m/z* 2530 corresponded to a N-glycan with 2 or 3 branches extended with 4-LacNAc-units or more (depending if it was bisected or not), while the ion at *m/z* 2775 corresponded to a bisected tetra-antennary N-glycan that had one branch extended with 3 LacNAc repeats while the rest were at least 4 LacNAc units long. Finally, the ions at *m/z* 1906, 2081, 2326 and 2571 corresponded to bi-, tri- and tetra-antennary N-glycans that had all of their branches extended with 4 LacNAc repeats or more. The above data suggest that a part of the resting and recently activated CTL clone F3.2 N-glycans had all their

branches extended with at least 4 LacNAc repeats.

In order to express the percent difference of the poly-LacNAc chains between the resting and the recently activated CTLs, we calculated the relative abundance of all the N-glycans with more than one terminal GlcNAc and compared it with the summed relative abundance of the ions at *m/z* 1141 and 1345 that corresponded to N-glycans with two LacNAc units or less. The results showed that compared with the resting, recently activated CTLs contained ~30% more N-glycans with one or more terminal GlcNAc N-glycans. Therefore, the data suggest that recently activated CTLs contained N-glycans with more branches of at least four LacNAc units.

We then performed GC-MS linkage analysis of the above resulting N-glycans where any possible variations in the levels of 2,4-linked mannose and 2,6-linked mannose would directly positively correlate with the abundance of tri- or/and tetra-antennary N-glycans, but specifically for those that were elongated with more than 4-LacNAc units. Our data showed that 2,4-linked mannose and 2,6-linked mannose increased by ~80% and 60% on the recently activated clone F3.2 CTLs (supplemental Table S1) suggesting that more branches of at least 4-LacNAc units were found on the recently activated CTLs than the resting CTLs. In addition, combining the data from the MALDI-TOF-MS that indicated that the most abundant structure corresponded to triply terminated GlcNAc N-glycan (*m/z* 2081) and the data from the GC-MS linkage analysis that the 2,4-linked mannose residue was more abundant than the 2,6-linked mannose residue, we concluded that the most abundant poly-LacNAc N-glycan corresponded to the tri-antennary N-glycan structures of GlcNAcβ1-2(GlcNAcβ1-4)Manβ1-3.

Recently activated CTLs have lower abundance of α2,6-linked NeuAc— Endo-β-galactosidase digestion suggested that, compared with the resting state, there was a decrease in the sialylation of the N-glycans in the recently activated state of both CTLs. However, the previous experiments did not reveal any information concerning the linkage of the NeuAc residues. Therefore, we applied α2-3 specific sialidase digestion on resting and recently activated CTL clone A10 in order to relatively quantify the ratio of α2,3-NeuAc/α2,6-NeuAc residues between these different conditions.

Fig. 7 depicts the MALDI-TOF mass spectra of permethylated N-glycans of CTL clone A10 in resting and recently activated states after sialidase-S (α2-3 specific) digestion. Comparing the ratio of sialylation to the base core fucosylated bi-antennary N-glycan (*m/z* 2244) we found that resting state CTL clone A10 was characterized by a high abundance of mono-sialylated (*m/*z 2605, 2850, 3054 and 3299) and di-sialylated (*m/*z 2966) N-glycans (Fig. 7*A*). On the contrary, the recently activated CTL clone A10 exhibited a lower abundance of mono- and di-sialylated N-glycans (Fig. 7*B*). These data suggest that the recently activated CTL clone A10 has N-glycans with lower abundance of α2,6-linked NeuAc residues than the resting state. This ratio was found to be ~106% lower in the recently activated CTLs.

The abundance of α2,6-linked NeuAc is directly correlated with the abundance of the 6-linked galactose residue. Therefore, we performed GC-MS linkage analysis on both the resting and recently activated CTL clone A10 in order to detect any possible difference in the abundance of 6-linked galactose residues. The results suggested that recently activated CTL clones A10 contained 56% less 6-linked galactose residue compared with their resting state (data not shown). Taken altogether, the data suggested that recently activated CTLs contained less α2,6-linked NeuAc residues than their resting state CTLs.

DISCUSSION

Defining the underlying immunosuppressive mechanisms of how tumor microenvironment impairs TIL function is of great importance. The level of galectins, abundant in solid tumors, has been correlated with the aggressiveness of the tumor and it has been hypothesized that they might modulate tumor progression and influence the disease outcome (19, 20). This suggestion appears to hold true because cells highly regulate the expression of endogenous galectins and their ligands in order to regulate cellular functions, suggesting that exogenous galectins or modification in the expression of galectin ligands could lead to pathology (21). The results presented here, have been obtained with clones and therefore are expected to be more rigorous than polyclonal splenocytes that may contain

different cell types. Applying ultra-sensitive MALDI-TOF-MS, combined with various glycosidase digestions and GC-MS linkage analyses, we make the novel observation that the N-glycome of the recently activated human $CD8^+$ CTLs, when compared with the N-glycome of the resting CTLs: (i) consists of longer LacNAc chains of which a portion are longer that four units ($(LacNAc)_4$, poly-LacNAcs); (ii) contains more branched (multi-antennary) N-glycans. These observations verify our working hypothesis that activation of human CTLs and TILs results in the expression of surface glycoproteins that exhibit higher abundance of galectin-3 ligands and possibly other galectin ligands such as galectin-1. This combined with the high abundance of extracellular galectin-3 found in tumor microenvironments could potentially explain the loss of TIL functions through a mechanism of reduced motility of surface molecules.

Galectin-3 is a β-galactoside binding lectin that binds to internal LacNAc repeats and it is not severely affected by the terminal epitopes at the non-reducing end of long-LacNAc extended glycans (22, 23). Therefore binding to the long poly-LacNAc chains is not affected by the variations of the abundance of sialic acids, sLe^x and Le^x epitopes found here. Thus, our data suggest that on the recently activated CTLs the increased abundance of LacNAc repeats increases the galectin-3-LacNAc interactions and blocks the mobilization of various glycoproteins. Simultaneously, galectin-3 is a lectin that possesses multivalent carbohydrate binding and cross-linking activity (24). Surprisingly, on the recently activated CTLs, these poly-LacNAc extensions were found to be more abundant on tri-antennary N-glycans with GlcNAcβ1-2(GlcNAcβ1-4)Manβ1-3(GlcNAcβ1-2Manβ1-6)Man branches and less abundant on tetra-antennary N-glycans, while resting CTLs exhibited reduced abundance of these tri- and tetra-antennary branches. Most interestingly, our data suggest that these poly-LacNAc repeats appeared to be mainly equally distributed on all available N-glycan branches and not selectively enriched on a specific N-glycan branch. The above suggest that recently activated human CTLs can form more multivalent galectin-3-LacNAc lattices, a fact that combined with the high levels of galectin-3 found in tumor microenvironments, could further explain the reduced motility of surface glycoproteins.

Our results are consistent with previous mouse studies highlighting the importance of N-glycosylation and specifically how LacNAc abundance and branching could block T cell activation by regulating the mobility of key surfaces molecules, such the TCR (9). However, those data suggested the selective extension of LacNAc repeats on the β1,6-GlcNAc branch, something that has not been verified from our data. Considering the data obtained here, it is possible that variations of LacNAc extensions are taking place on all available branches of mouse N-glycans, but only variations of the β1,6-branch were detected by the *Phaseolus vulgaris* leukoagglutinin binding lectin (9, 25). The possibility that mouse TCR is specifically decorated either with tri-antennary N-glycans of type GlcNAcβ1-2(GlcNAcβ1-6)Manβ1-6Man or tetra-antennary N-glycans, cannot be excluded. In such a case, a possible down-regulation of the *Mgat5* gene would provoke a reduced abundance of the LacNAc "density" which is expected to decrease the galectin-3-LacNAc lattices.

A major surface glycoprotein that could be affected from the above galectin-3-LacNAc lattices is the TCR. In the recently activated human CTLs, characterized by the loss of effector functions and the absence of co-localization of TCR and CD8, the TCR was found in close proximity to galectin-3. A treatment of these CTL with galectin ligands (LacNAc) resulted within 2 h in TCR/CD8 co-localization, detaching the galectin-3 from the TCR and was accompanied by restored functions (8). This suggests that galectin-3, which is involved in distancing the TCR from CD8 (8), could potentially regulate CTLs functions. Several lines of evidence support this concept meaning that loss of effector functions on human CTLs could be associated with the galectin-3-LacNAc-TCR lattices. First, treatment of human TIL with anti-galectin-3 antibody detached galectin-3 from cells and boosted their functions (6). Second, human TCR α-chain, in contrast to β-chain, has been shown to be occupied exclusively by complex N-glycans (26). Third, a previous study showed that the removal of a N-glycosylation site from the human TCR α-chain, resulted in improved sensitivity of a T cell response (functional avidity) (11). Finally and most importantly, a key step in T cell effector function is the phosphorylation of

immunoreceptor tyrosine-based activation motifs (ITAMs) within the CD3 complex, which in turn is depended on LCK activation (27). However, a recent study has shown that LCK is already activated in resting human T cells, enough to initiate TCR signaling (28). Moreover, the expression-activation of LCK did not appear to depend on TCR or co-receptor expression-contact with pMHC. Hence, the above collectively suggest that the increased galectin-3-LacNAc lattices occurring in the recently activated CTLs and accompanied by the loss of effector functions could be linked, though not exclusively, to the de-localization of the TCR from the CD8 molecule. This in turn could potentially prevent the ITAMs phosphorylation by keeping the TCR-CD3 complex distant from LCK, which is stably associated with the CD8 co-receptor (29) and therefore prevent further signaling. This concept has been already been shown in mouse studies. *Mgat5*-deficient mice after stimulation exhibited increased association of the Zap-70 kinase with ITAMs, compared with WT mice, exhibiting a negative regulation of galectin-3-LacNAc lattices and ITAM phosphorylation (9).

Our data showed that the changes in LacNAc abundance between the resting and recently activated states of clone F3.2 were less prominent than those of clone A10. For TILs present in a tumor microenvironment of a given concentration of galectins and activated by the same peptide-MHC complex, the ones with a smaller increase in LacNAc abundance (such as clone F3.2) would be expected to present a relatively higher motility of surface molecules such as the TCR, compared to other TILs with a more pronounced increase in LacNAc abundance (such as of clone A10). This is because the reduced increase of LacNAc abundance should induce a reduced increase of galectin-3-LacNAc lattices and therefore should have a smaller impact on the motility of surface molecules. Hence, a reduced increase of LacNAc abundance in activated T cells would be expected to result in higher motility of surface molecules and possibly effector functions. This concept has already been proposed in a previous study suggesting that either the peptide-MHC complexes that would be predicted to overcome the negative regulation by the galectin lattice, or the reduced N-glycan branching that would reduce the interaction of TCR for galectin would lead to activation (30).

Our data showed that recently activated human $CD8^+$ CTL clones exhibited a lower abundance of terminal α2,6-linked NeuAc residues than resting CTLs. This fact is expected to affect galectin-1-glycoprotein binding interactions. Galectin-1 binds to terminal LacNAc units either in their unmodified state or when they are decorated with α2,3-linked NeuAc (31, 32), but this binding is blocked by α2,6-linked NeuAc (23, 33, 34). Therefore, our data suggest that more galectin-1-ligand binding interactions are expected to be formed in recently activated CTLs than in the resting CTLs. Interactions of the TCR with galectin-1, instead of galectin-3, that may contribute to lattice formation and restrain TCR function, cannot be excluded either. Indeed, we detected extracellular galectin-1, in addition to galectin-3 and both have been detected in TILs (6). However, in a previous study, the anti-galectin-3 monoclonal antibody B2C10, while being able to boost TIL function, seemed unable to detach galectin-1, suggesting that detaching galectin-3 from TIL was sufficient to restore function, while not excluding the contribution of other galectins (6). Exactly how and if this could be related to loss of effector functions, related to TCR, on the recently activated human CTLs is currently unknown. Moreover, the possibility of additional molecules that contribute to the mechanism, such as the CD45, with galectin-1 and/or galectin-3, cannot be excluded either (35, 36). In mouse, the decreased abundance of α2,6-linked sialic acids has been described in $CD4^+$ and $CD8^+$ T lymphocytes during activation and it has been suggested that this leads to increased binding with CD22 (siglec-2) and/or galectin-1 (13).

MALDI-TOF-MS suggested that O-glycans of recently activated human CTLs exhibited increased abundance of disialylated core 1 and monosialylated core 2 structures than the resting CTLs. The increased abundance of core 2 O-glycans on recently activated CTLs is in accordance with previous studies showing increased abundance of core 2 O-glycans in human leukosialin after activation of human T cells (37). Exactly how and if changes in O-glycosylation could be related to loss of effector functions in the recently activated human CTLs is currently unknown. Noteworthy, when our CTLs were activated and cultured for 4 days in the presence of swainsonine, an inhibitor of mannosidase II, neither their functions nor the

TCR-CD8 co-localization were lost (8). Previous studies have shown that changes in O-glycan structures could affect CD8 co-receptor signaling by either altering the conformation of its stalk region (38-40) or by regulating its avidity (41). Further studies will show if O-glycosylation affects the loss of effector functions.

In conclusion, our results show that the N-glycome of the recently activated CTL clones, after antigenic stimulation, result in increased abundance-"density"- of poly-LacNAc chains that is able to sustain galectin-3 lattices, without excluding the participation of other galectins, and reduce the motility of key surface molecules, such as the TCR that is accompanied by the loss of effector functions of TIL. The possibility that certain surface glycoproteins do not follow the alteration of glycosylation presented here cannot, however, be excluded either.

REFERENCES

1. Boon, T., Coulie, P. G., Van den Eynde, B. J., and van der Bruggen, P. (2006) *Annu. Rev. Immunol.* **24**, 175–208
2. Wieërs, G., Demotte, N., Godelaine, D., and van der Bruggen, P. (2011) *Cancers* **3**, 2904–2954
3. Van den Hove, L. E., Van Gool, S. W., Van Poppel, H., Baert, L., Coorevits, L., Van Damme, B., and Ceuppens, J. L. (1997) *Clin. Exp. Immunol.* **109**, 501–509
4. Zippelius, A., Batard, P., Rubio-Godoy, V., Bioley, G., Liénard, D., Lejeune, F., Rimoldi, D., Guillaume, P., Meidenbauer, N., Mackensen, A., Rufer, N., Lubenow, N., Speiser, D., Cerottini, J.-C., Romero, P., and Pittet, M. J. (2004) *Cancer Res.* **64**, 2865–2873
5. Harlin, H., Kuna, T. V., Peterson, A. C., Meng, Y., and Gajewski, T. F. (2006) *Cancer Immunol. Immunother.* **55**, 1185–1197
6. Demotte, N., Wieers, G., Van Der Smissen, P., Moser, M., Schmidt, C., Thielemans, K., Squifflet, J. L., Weynand, B., Carrasco, J., Lurquin, C., Courtoy, P. J., and van der Bruggen, P. (2010) *Cancer Res.* **70**, 7476–7488
7. Wang, S.-F., Fouquet, S., Chapon, M., Salmon, H., Regnier, F., Labroquère, K., Badoual, C., Damotte, D., Validire, P., Maubec, E., Delongchamps, N. B., Cazes, A., Gibault, L., Garcette, M., Dieu-Nosjean, M.-C., Zerbib, M., Avril, M.-F., Prévost-Blondel, A., Randriamampita, C., Trautmann, A., and Bercovici, N. (2011) *PLoS ONE* **6**, e17621
8. Demotte, N., Stroobant, V., Courtoy, P. J., Van Der Smissen, P., Colau, D., Luescher, I. F., Hivroz, C., Nicaise, J., Squifflet, J.-L., Mourad, M., Godelaine, D., Boon, T., and van der Bruggen, P. (2008) *Immunity* **28**, 414–424
9. Demetriou, M., Granovsky, M., Quaggin, S., and Dennis, J. W. (2001) *Nature* **409**, 733–739
10. Togayachi, A., Kozono, Y., Ishida, H., Abe, S., Suzuki, N., Tsunoda, Y., Hagiwara, K., Kuno, A., Ohkura, T., Sato, N., Sato, T., Hirabayashi, J., Ikehara, Y., Tachibana, K., and Narimatsu, H. (2007) *Proc. Natl. Acad. Sci. U.S.A.* **104**, 15829–15834
11. Kuball, J., Hauptrock, B., Malina, V., Antunes, E., Voss, R. H., Wolfl, M., Strong, R., Theobald, M., and Greenberg, P. D. (2009) *J. Exp. Med.* **206**, 463–475
12. Joo, H. G., Goedegebuure, P. S., Sadanaga, N., Nagoshi, M., Bernstorff, von, W., and Eberlein, T. J. (2001) *J. Leukoc. Biol.* **69**, 555–564
13. Comelli, E. M., Sutton-Smith, M., Yan, Q., Amado, M., Panico, M., Gilmartin, T., Whisenant, T., Lanigan, C. M., Head, S. R., Goldberg, D., Morris, H. R., Dell, A., and Paulson, J. C. (2006) *J. Immunol.* **177**, 2431–2440
14. Antonopoulos, A., North, S. J., Haslam, S. M., and Dell, A. (2011) *Biochem. Soc. Trans.* **39**, 1334–1340
15. Jang-Lee, J., North, S. J., Sutton-Smith, M., Goldberg, D., Panico, M., Morris, H., Haslam, S., and Dell, A. (2006) *Meth. Enzymol.* **415**, 59–86
16. Nakagawa, H., Yamada, T., Chien, J. L., Gardas, A., Kitamikado, M., Li, S. C., and Li, Y. T. (1980) *J. Biol. Chem.* **255**, 5955–5959
17. Fukuda, M. N. (1981) *J. Biol. Chem.* **256**, 3900–3905
18. Ceroni, A., Maass, K., Geyer, H., Geyer, R., Dell, A., and Haslam, S. M. (2008) *J. Proteome Res.* **7**, 1650–1659

19. Liu, F.-T., and Rabinovich, G. A. (2005) *Nat. Rev. Cancer* **5**, 29–41
20. Rabinovich, G. A., and Toscano, M. A. (2009) *Nat. Rev. Immunol.* **9**, 338–352
21. Dam, T. K., and Brewer, F. C. (2010) *Glycobiology* **20**, 1061–1064
22. Hirabayashi, J., Hashidate, T., Arata, Y., Nishi, N., Nakamura, T., Hirashima, M., Urashima, T., Oka, T., Futai, M., Muller, W. E. G., Yagi, F., and Kasai, K.-I. (2002) *Biochim. Biophys. Acta* **1572**, 232–254
23. Stowell, S. R., Arthur, C. M., Mehta, P., Slanina, K. A., Blixt, O., Leffler, H., Smith, D. F., and Cummings, R. D. (2008) *J. Biol. Chem.* **283**, 10109–10123
24. Ahmad, N., Gabius, H.-J., André, S., Kaltner, H., Sabesan, S., Roy, R., Liu, B., Macaluso, F., and Brewer, C. F. (2004) *J. Biol. Chem.* **279**, 10841–10847
25. Cummings, R. D., and Kornfeld, S. (1982) *J. Biol. Chem.* **257**, 11230–11234
26. Clevers, H., Alarcon, B., Wileman, T., and Terhorst, C. (1988) *Ann. Rev. Immunol.* **6**, 629–662
27. Friedl, P., Boer, den, A. T., and Gunzer, M. (2005) *Nat. Rev. Immunol.* **5**, 532–545
28. Nika, K., Soldani, C., Salek, M., Paster, W., Gray, A., Etzensperger, R., Fugger, L., Polzella, P., Cerundolo, V., Dushek, O., Höfer, T., Viola, A., and Acuto, O. (2010) *Immunity* **32**, 766–777
29. Barber, E. K., Dasgupta, J. D., Schlossman, S. F., Trevillyan, J. M., and Rudd, C. E. (1989) *Proc. Natl. Acad. Sci. U.S.A.* **86**, 3277–3281
30. Chen, I.-J., Chen, H.-L., and Demetriou, M. (2007) *J. Biol. Chem.* **282**, 35361–35372
31. Pace, K., Lee, C., Stewart, P., and Baum, L. (1999) *J. Immunol.* **163**, 3801–3811
32. Leppänen, A., Stowell, S., Blixt, O., and Cummings, R. D. (2005) *J. Biol. Chem.* **280**, 5549–5562
33. Lobsanov, Y., Gitt, M., and Leffler, H. (1993) *J. Biol. Chem.* **268**, 27034–22738
34. Earl, L. A., Bi, S., and Baum, L. G. (2010) *J. Biol. Chem.* **285**, 2232–2244
35. Irles, C., Symons, A., Michel, F., Bakker, T. R., van der Merwe, P. A., and Acuto, O. (2003) *Nat. Immunol.* **4**, 189–197
36. Sato, T., Furukawa, K., Autero, M., Gahmberg, C. G., and Kobata, A. (1993) *Biochemistry* **32**, 12694–12704
37. Piller, F., Piller, V., Fox, R. I., and Fukuda, M. (1988) *J. Biol. Chem.* **263**, 15146–15150
38. Moody, A. M., Chui, D., Reche, P. A., Priatel, J. J., Marth, J. D., and Reinherz, E. L. (2001) *Cell* **107**, 501–512
39. Daniels, M. A., Devine, L., Miller, J. D., Moser, J. M., Lukacher, A. E., Altman, J. D., Kavathas, P., Hogquist, K. A., and Jameson, S. C. (2001) *Immunity* **15**, 1051–1061
40. Moody, A. M., North, S. J., Reinhold, B., Van Dyken, S. J., Rogers, M. E., Panico, M., Dell, A., Morris, H. R., Marth, J. D., and Reinherz, E. L. (2003) *J. Biol. Chem.* **278**, 7240–7246
41. Merry, A. H., Gilbert, R. J. C., Shore, D. A., Royle, L., Miroshnychenko, O., Vuong, M., Wormald, M. R., Harvey, D. J., Dwek, R. A., Classon, B. J., Rudd, P. M., and Davis, S. J. (2003) *J. Biol. Chem.* **278**, 27119–27128

Acknowledgements—We are grateful for support from the Biotechnology and Biological Sciences Research Council (B19088 and BBF0083091 to A.D. and S.M.H.). This work was also supported by grants from the Fondation contre le Cancer (Belgium) and Fonds de la Recherche Scientifique Médicale (Belgium) (P.B.).

FOOTNOTES

[1]To whom correspondence should be addressed: Anne Dell, Division of Molecular Biosciences, Imperial College London, South Kensington Campus, SW7 2AZ, UK, Tel.: +44 (0)207 5945219; E-mail: a.dell@imperial.ac.uk

[2]The abbreviations used are: CTL, cytolytic T lymphocyte; HF, hydrofluoric acid; LacNAc, Galβ1,4GlcNAc; Le^X, Galβ1,4(Fucα1,3)GlcNAc; PMAA, partially methylated alditol acetates; sLe^X, NeuAcα2,3Galβ1,4(Fucα1,3)GlcNAc; TIL, tumor-infiltrating T lymphocyte

FIGURE LEGENDS

FIGURE 1. **LacNAc treatment of human CTL can restore their ability to secrete IFN-γ.** Resting CTL clones were expanded by stimulation every two weeks with peptide-pulsed EBV-B cells, in the presence of feeder cells and IL-2. To assess effector functions, 10,000 CTL were collected, either at the resting state (± two weeks after stimulation) or in an activated state (four days after stimulation). CTL were incubated (or not) for 2 h with LacNAc (2 mM) and subsequently stimulated with peptide-pulsed HLA-A1 cells. IFN-γ was measured by ELISA in the supernatant of overnight cocultures.

FIGURE 2. **MALDI-TOF mass spectra of permethylated N-glycans of CTL clone A10 derived from resting and recently activated state.** N-glycomic profiles of *A*, resting; and *B*, recently activated CTL clone A10 were obtained from the 50% MeCN fraction from a C_{18} Sep-Pak column ("Experimental Procedures"). Annotated structures are according to the Consortium for Functional Glycomics (http://www.functionalglycomics.org) guidelines. All molecular ions are $[M+Na]^+$. Putative structures based on composition, tandem MS and the biosynthetic knowledge. Structures that show sugars outside a bracket have not been unequivocally defined.

FIGURE 3. **MALDI-TOF mass spectra of permethylated O-glycans of CTL clone A10 derived from resting and recently activated state.** O-glycomic profiles of *A*, resting; and *B,* recently activated CTL clone A10 were obtained from the 35% MeCN fraction from a C_{18} Sep-Pak column ("Experimental Procedures"). Annotated structures are according to the Consortium for Functional Glycomics (http://www.functionalglycomics.org) guidelines. All molecular ions are $[M+Na]^+$. Putative structures based on composition, tandem MS and the biosynthetic knowledge.

FIGURE 4. **Low mass MALDI-TOF spectra of permethylated N-glycans derived from endo-β-galactosidase digestion of resting and recently activated CTL clone A10.** N-glycomic profiles of CTL clone A10 in *A*, resting; and *B*, recently activated states. Profiles of N-glycans are from the 35% MeCN fraction from a C_{18} Sep-Pak ("Experimental Procedures"). All molecular ions are $[M+Na]^+$. Putative structures based on composition, tandem mass spectrometry and the literature shown. Annotated structures are according to the Consortium for Functional Glycomics (http://www.functionalglycomics.org) guidelines. Not annotated peaks correspond to non-glycan structures or to matrix peaks.

FIGURE 5. **Middle mass MALDI-TOF spectra of permethylated N-glycans derived from endo-β-galactosidase digestion of resting and recently activated CTL clone A10.** N-glycomic profiles of CTL clone A10 in *A*, resting; and *B*, recently activated states. Profiles of N-glycans are from the 35% MeCN fraction from a C_{18} Sep-Pak ("Experimental Procedures"). All molecular ions are $[M+Na]^+$. Putative structures based on composition, tandem mass spectrometry and the literature shown. Annotated structures are according to the Consortium for Functional Glycomics (http://www.functionalglycomics.org) guidelines.

FIGURE 6. **Long polylactosamine units are more abundant on recently activated CTL clone F3.2 N-glycans.** *A*, Expected resulting N-glycans of resting and recently activated CTLs after HF and sialidase treatments (*upper panel* structure) and additionally after two consecutive cycles of galactosidase (G) and β-*N*-acetylhexosaminidase (H) treatments and one endo-β-galactosidase (endo) treatment (*lower panel* structure). *B*, N-glycomic profile of CTL clone F3.2 of resting (*upper panel*) and recently activated states (*lower panel*). Profiles of N-glycans are from the 50% MeCN fraction from a C_{18} Sep-Pak. All molecular ions are $[M+Na]^+$. Putative structures based on composition, tandem mass spectrometry and the literature shown. Annotated structures are according to the Consortium for Functional Glycomics (http://www.functionalglycomics.org) guidelines. Note that the most abundant long polylactosamine units (higher than 4 LacNAc units long) are found at *m/z* 2081 that corresponds to a tri-antinnary N-glycan structure.

FIGURE 7. **Recently activated CTL clone A10 contains less α2,6-linked NeuAc residues than the resting CTL.** Partial MALDI-TOF mass spectra of permethylated N-glycans derived from *A*, resting; and *B*, recently activated CTL clone A10 after treatment with sialidase-S (α2-3 specific). N-glycomic profiles were obtained from the 50% MeCN fraction from a C_{18} Sep-Pak column ("Experimental Procedures"). All molecular ions are $[M+Na]^+$. Putative structures based on composition, tandem MS and the literature shown. Annotated structures are according to the Consortium for Functional Glycomics (http://www.functionalglycomics.org) guidelines.

TABLES

TABLE 1. GC-MS linkage analyses of partially methylated alditol acetates obtained from the PNGase F released N-linked glycans of CTL clones A10 and F3.2. Desialylated (Sialidase-A, non-specific) permethylated N-glycans were hydrolyzed, reduced, acetylated and analyzed by GC-MS (see "Experimental Procedures").

CTL clones	Relative abundance[a]			% Difference (on activated)[b]		
	3-Gal	4-GlcNAc	3,4-GlcNAc	3-Gal	4-GlcNAc	3,4-GlcNAc
	Resting R. Activated	Resting R. Activated	Resting R. Activated			
A10	0.279 0.616	0.086 0.382	0.008 0.037	**+121%**	**+344%**	**+363%**
F3.2	0.273 0.403	0.184 0.311	0.024 0.031	**+48%**	**+69%**	**+29%**

[a]Upper panel values express the resting state CTLs relative abundance; lower panel values express the recently activated CTLs relative abundance. Relative abundance of 3-linked Gal, 4-linked GlcNAc and 3,4-linked GlcNAc were obtained normalizing the integrated area peak of the extracted ion current (XIC) chromatogram of a specific residue to the summed integrated areas of the XICs of 3,6-linked mannose and 3,4,6-linked mannose.

[b]Percent difference of the relative abundance between resting and recently activated CTL clones, (recently activated - resting)/resting%.

Figure 1

IFN-γ secreted by 10,000 T cells upon stimulation (pg/ml)

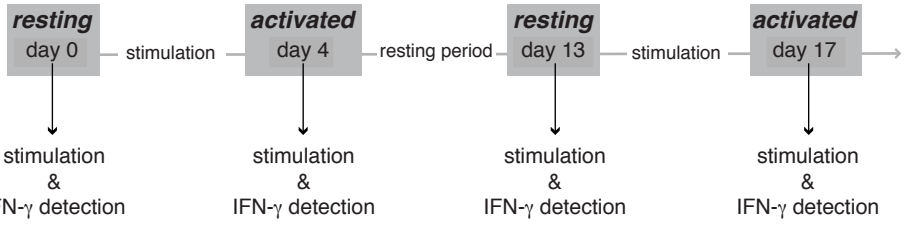

clone A10	non-treated	*580±27*	*150±12*	*2016±83*	*0*
	LacNAc		*686±38*		*1360±16*
clone F3.2	non-treated	*2007±140*	*410±41*		
	LacNAc		*1629±1*		

Figure 2

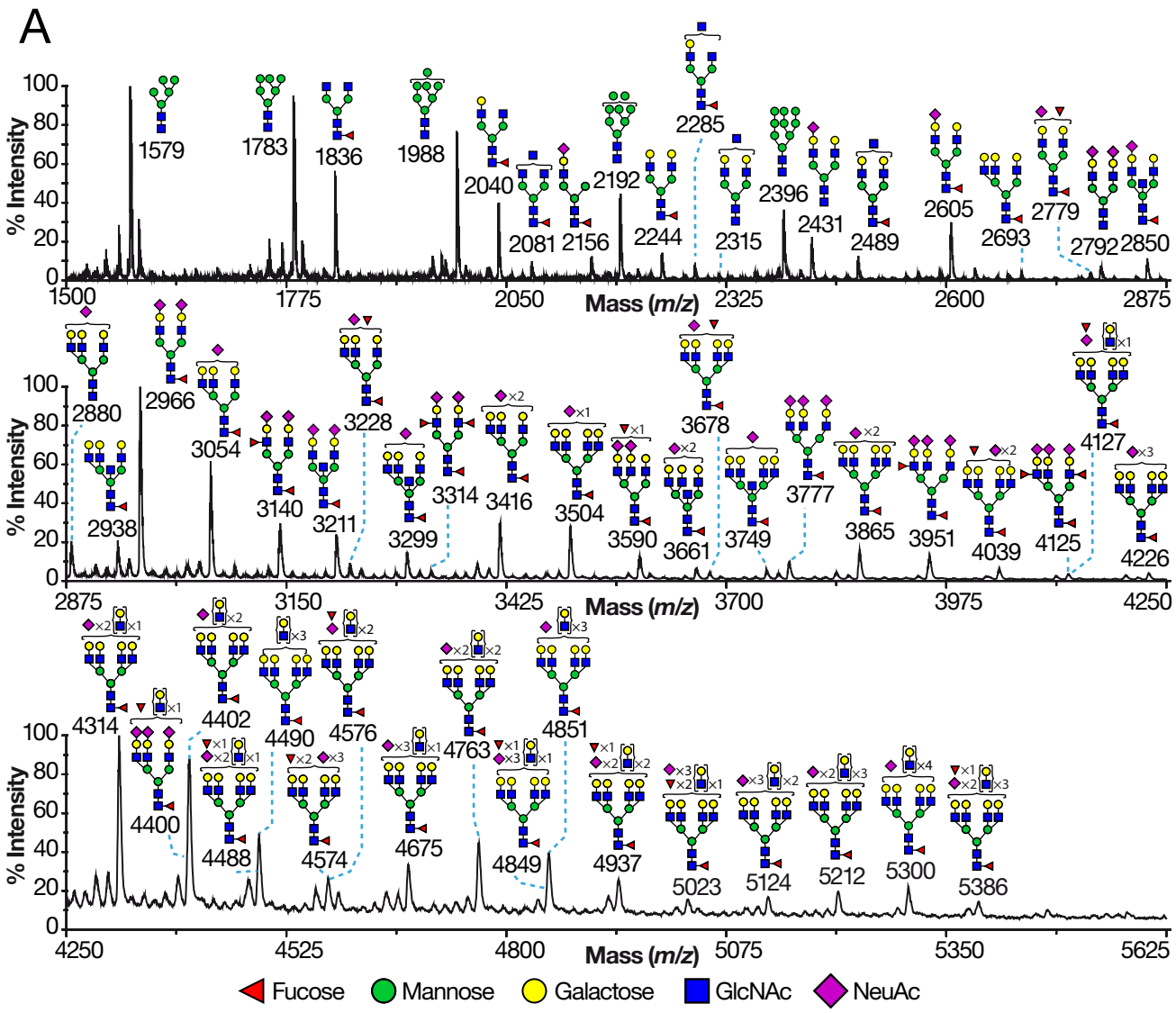
A
% Intensity
Mass (m/z)
1579
1783
1836
1988
2040
2081
2156
2192
2244
2285
2315
2396
2431
2489
2605
2693
2779
2792
2850
2880
2938
2966
3054
3140
3211
3228
3299
3314
3416
3504
3590
3661
3678
3749
3777
3865
3951
4039
4125
4127
4226
4314
4400
4402
4488
4490
4574
4576
4675
4763
4849
4851
4937
5023
5124
5212
5300
5386
Fucose
Mannose
Galactose
GlcNAc
NeuAc

Figure 2

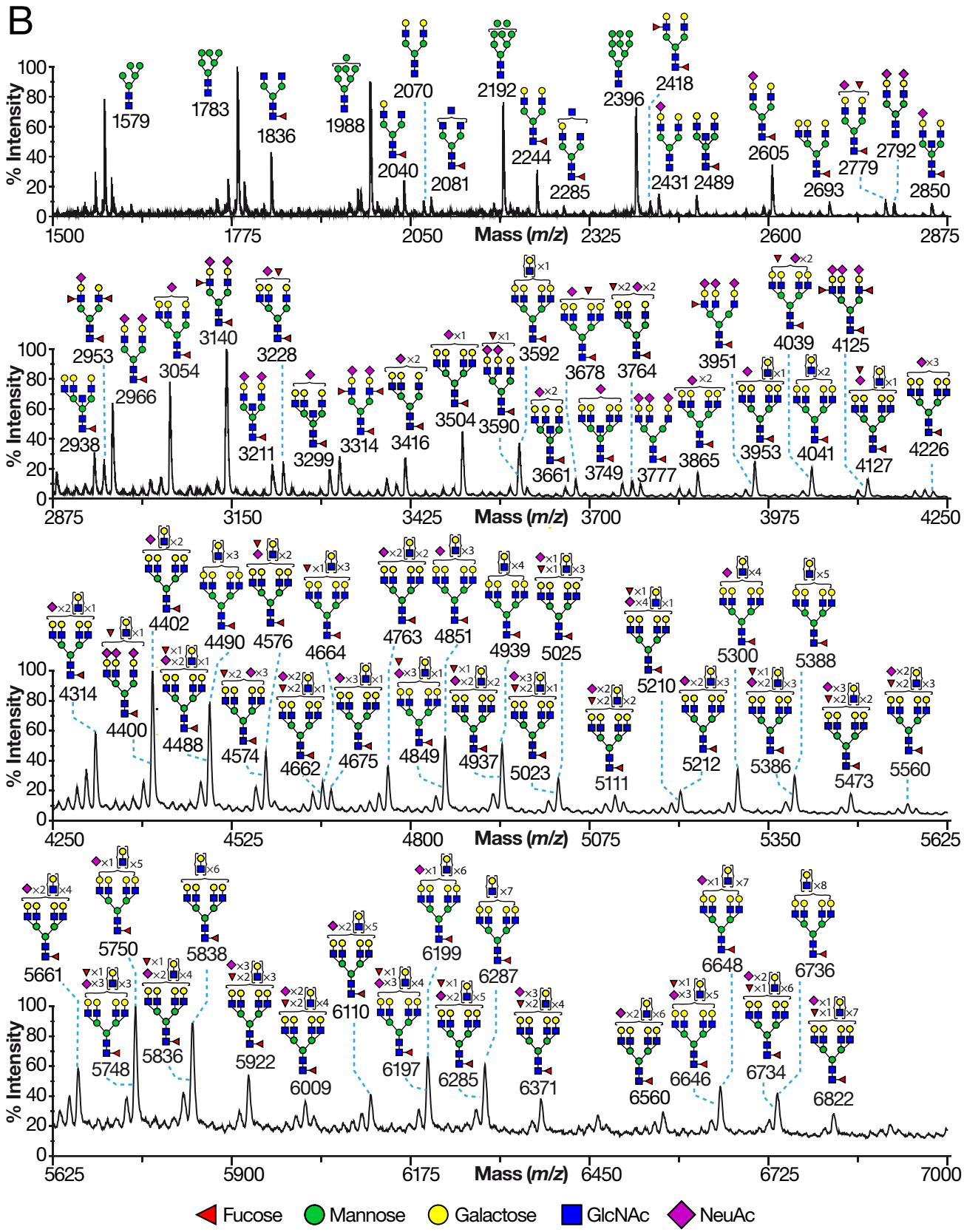
B
% Intensity
Mass (m/z)
1579
1783
1836
1988
2070
2040
2081
2192
2244
2285
2396
2418
2431
2489
2605
2693
2779
2792
2850
2953
2966
3054
3140
3228
2938
3211
3299
3314
3416
3504
3590
3592
3661
3678
3749
3764
3777
3865
3951
3953
4039
4041
4125
4127
4226
4314
4400
4402
4488
4490
4574
4576
4662
4664
4675
4763
4849
4851
4937
4939
5023
5025
5111
5210
5212
5300
5386
5388
5473
5560
5661
5748
5750
5836
5838
5922
6009
6110
6197
6199
6285
6287
6371
6560
6646
6648
6734
6736
6822
Fucose
Mannose
Galactose
GlcNAc
NeuAc

Figure 3

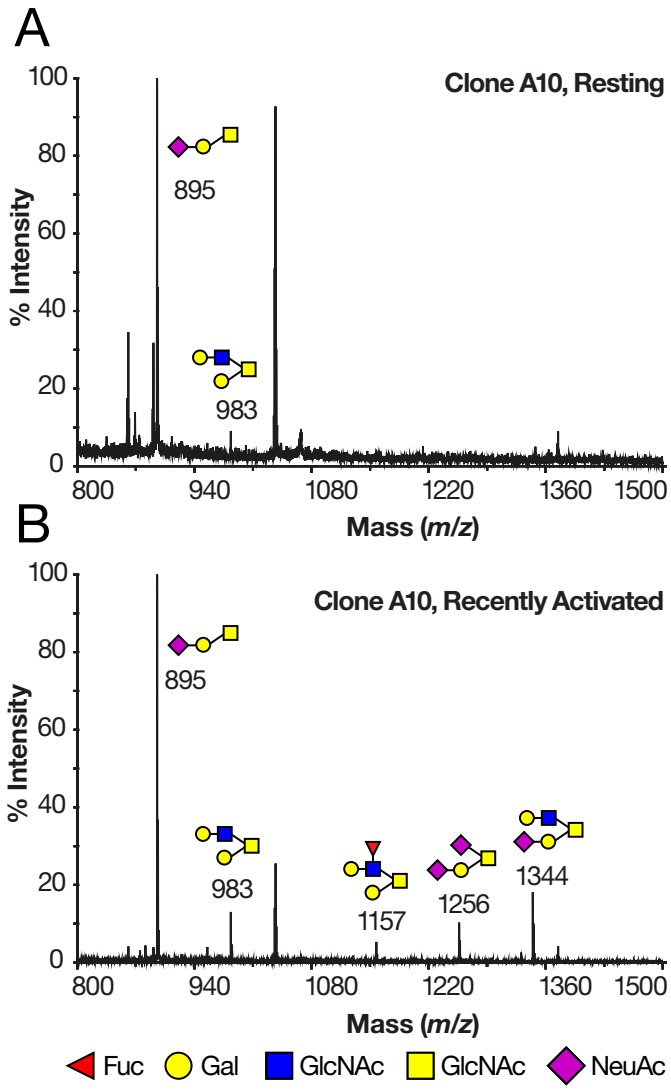
A
Clone A10, Resting
% Intensity
100
80
60
40
20
0
895
983
800
940
1080
1220
1360
1500
Mass (m/z)
B
Clone A10, Recently Activated
% Intensity
895
983
1157
1256
1344
Mass (m/z)
Fuc
Gal
GlcNAc
GlcNAc
NeuAc

Figure 4

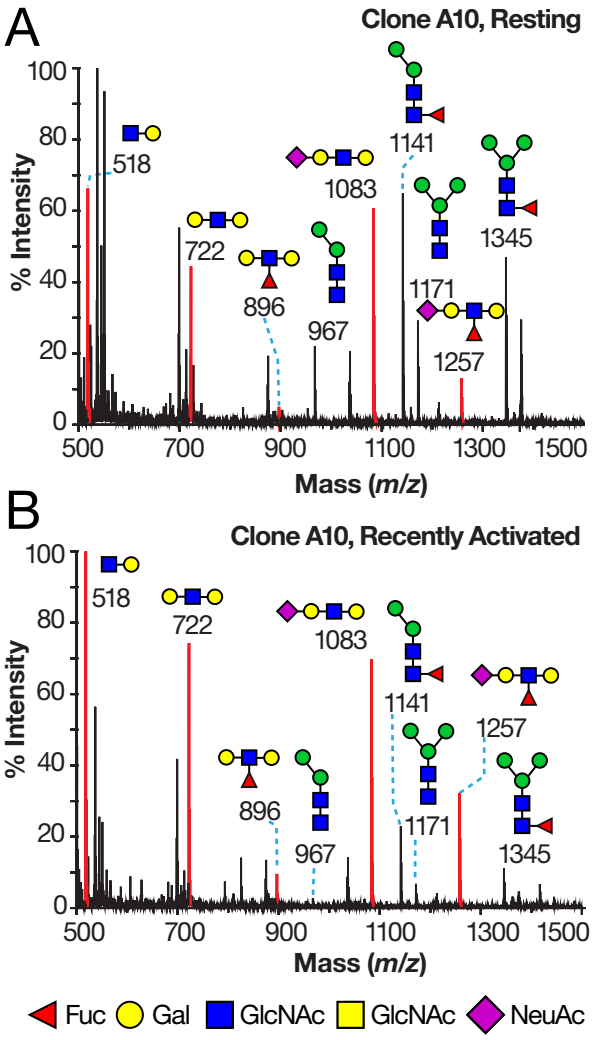
A
Clone A10, Resting
% Intensity
100
80
60
40
20
0
518
722
896
967
1083
1141
1171
1257
1345
500
700
900
1100
1300
1500
Mass (m/z)
B
Clone A10, Recently Activated
% Intensity
518
722
896
967
1083
1141
1171
1257
1345
Mass (m/z)
Fuc
Gal
GlcNAc
GlcNAc
NeuAc

Figure 5

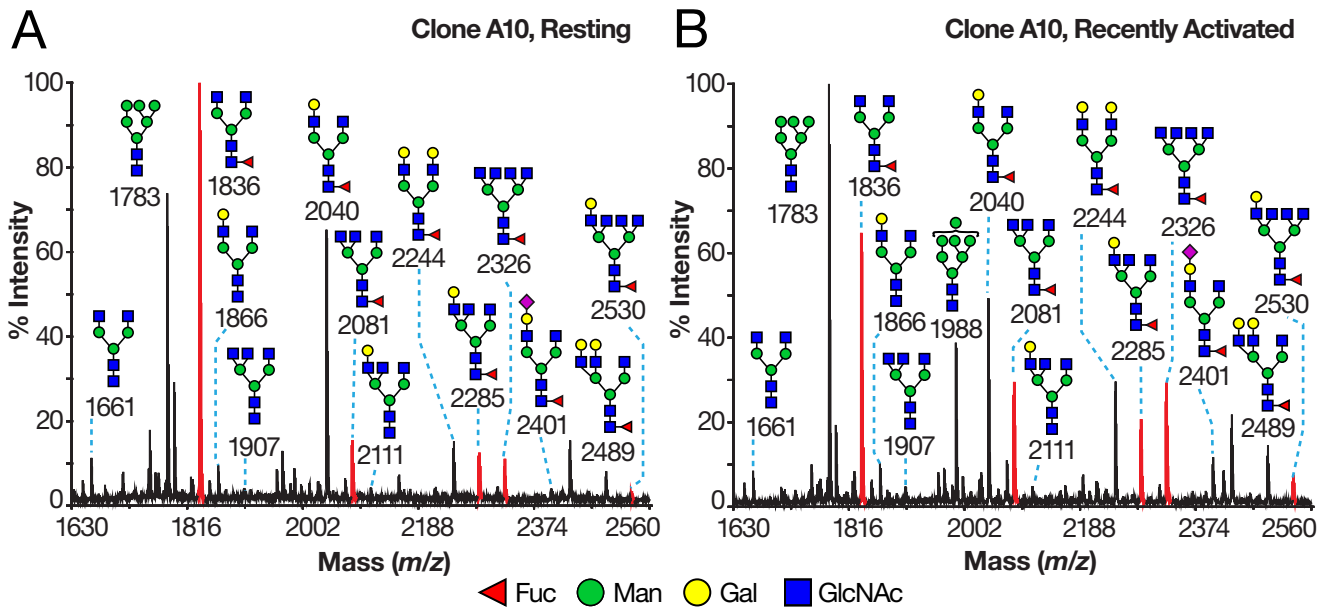
A
Clone A10, Resting
B
Clone A10, Recently Activated
% Intensity
100
80
60
40
20
0
1630
1816
2002
2188
2374
2560
Mass (m/z)
1661
1783
1836
1866
1907
2040
2081
2111
2244
2285
2326
2401
2489
2530
1988
Fuc
Man
Gal
GlcNAc

Figure 6

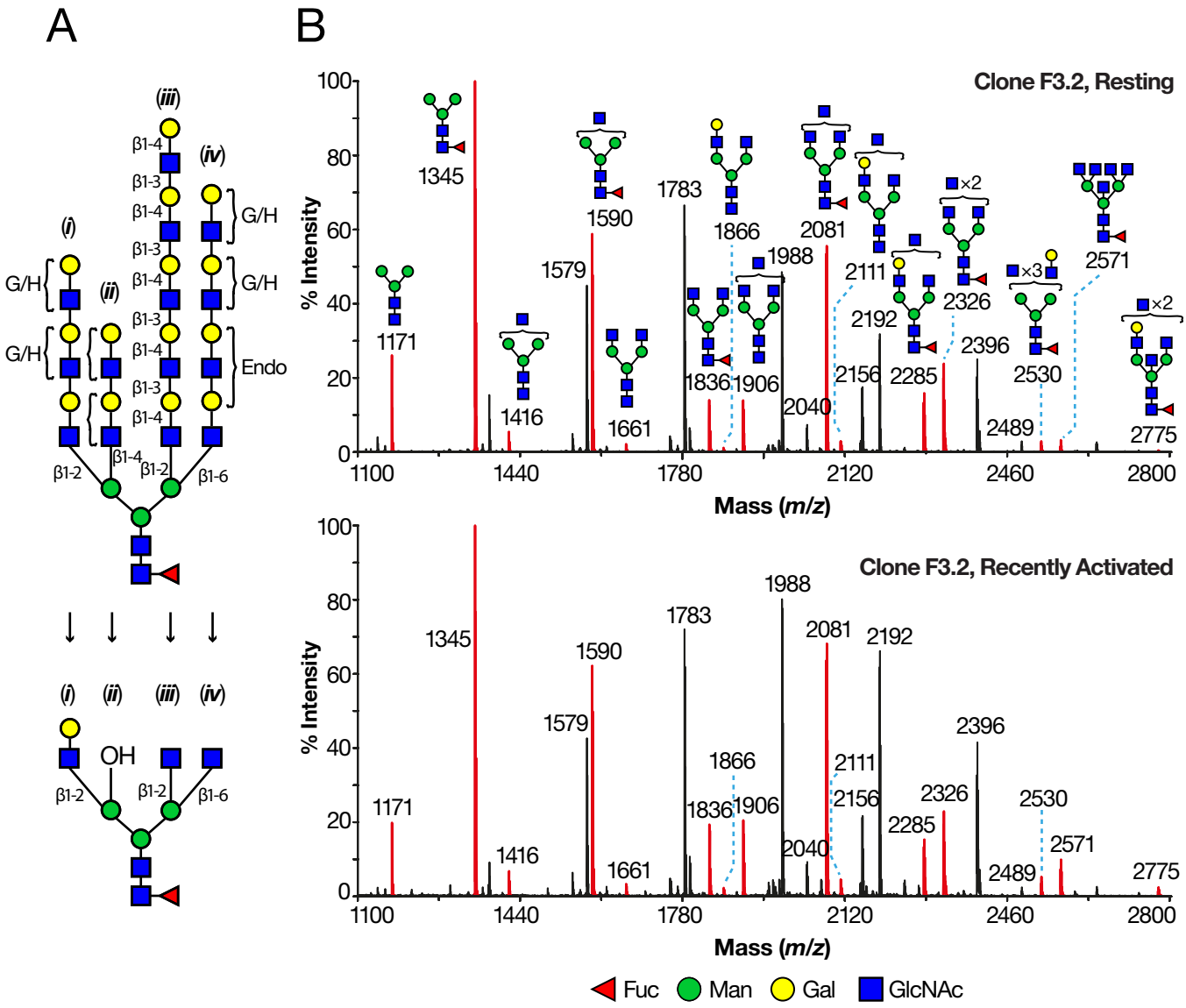
A
B
(i)
(ii)
(iii)
(iv)
G/H
G/H
G/H
Endo
β1-4
β1-3
β1-2
β1-6
OH
Clone F3.2, Resting
Clone F3.2, Recently Activated
% Intensity
Mass (m/z)
1345
1171
1416
1590
1579
1661
1783
1866
1836
1906
1988
2040
2081
2111
2192
2156
2285
2326
2396
2489
2530
2571
2775
×2
×3
Fuc
Man
Gal
GlcNAc

Figure 7

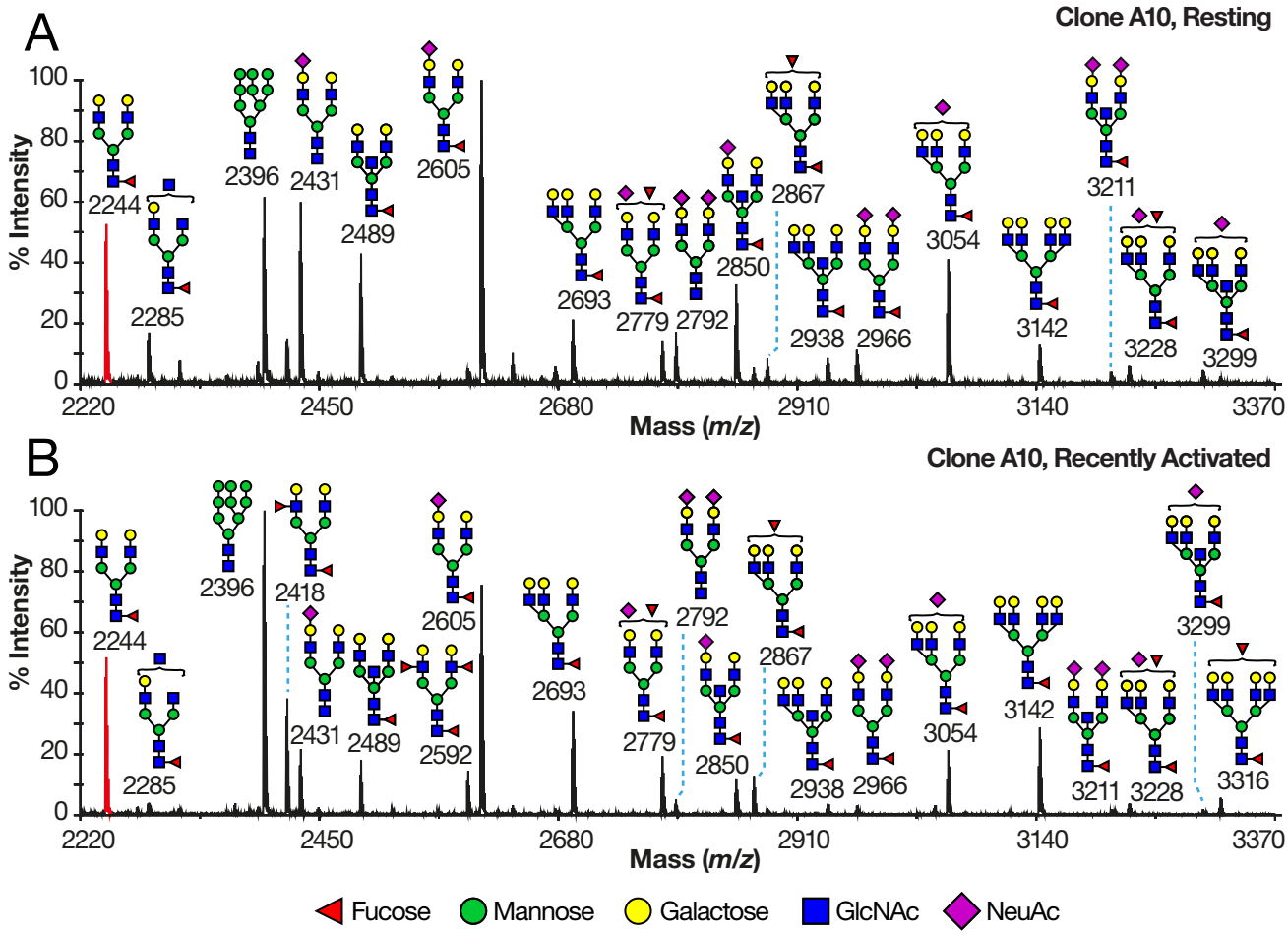
A
Clone A10, Resting
% Intensity
100
80
60
40
20
0
2244
2285
2396
2431
2489
2605
2693
2779
2792
2850
2867
2938
2966
3054
3142
3211
3228
3299
2220
2450
2680
2910
3140
3370
Mass (m/z)
B
Clone A10, Recently Activated
% Intensity
2244
2285
2396
2418
2431
2489
2592
2605
2693
2779
2792
2850
2867
2938
2966
3054
3142
3211
3228
3299
3316
2220
2450
2680
2910
3140
3370
Mass (m/z)
Fucose
Mannose
Galactose
GlcNAc
NeuAc